NASA/TM—2000–209891, Vol. 171

# Technical Report Series on the Boreal Ecosystem-Atmosphere Study (BOREAS)

*Forrest G. Hall and Andrea Papagno, Editors*

## Volume 171

## BOREAS TE-17 Production Efficiency Model Images

*Scott J. Goetz, Samual N. Goward, Stephen D. Prince, Kevin Czajkowski, and Ralph O. Dubayah*
*University of Maryland, College Park*

National Aeronautics and
Space Administration

**Goddard Space Flight Center**
Greenbelt, Maryland 20771

October 2000

Available from:

NASA Center for AeroSpace Information
7121 Standard Drive
Hanover, MD 21076-1320
Price Code: A17

National Technical Information Service
5285 Port Royal Road
Springfield, VA 22161
Price Code: A10

# BOREAS TE-17 Production Efficiency Model Images

Scott J. Goetz, Samual N. Goward, Stephen D. Prince, Kevin Czajkowski, Ralph Dubayah

## Summary

A BOREAS version of the Global Production Efficiency Model (http://www.inform.umd.edu/glopem/) was developed by TE-17 to generate maps of gross and net primary production, autotrophic respiration, and light use efficiency for the BOREAS region. This document provides basic information on the model and how the maps were generated. The data generated by the model are stored in binary image-format files.

Note that the files of this data set on the BOREAS CD-ROMs have been compressed using the Gzip program. See Section 8.2 for details.

## Table of Contents



## 1. Data Set Overview

### 1.1 Data Set Identification

BOREAS TE-17 Production Efficiency Model Images

### 1.2 Data Set Introduction

The Boreal Forest Production Efficiency Model (Boreal-PEM) is composed of a suite of models that provide estimates of the variables needed to drive a production efficiency model (i.e., one based on restrictions in the conversion "efficiency" of absorbed photosynthetically active radiation (APAR) in terms of unstressed gross primary production (GPP) through short-term environmental physiology).

### 1.3 Objective/Purpose

The purpose of the production efficiency modeling for the BOReal Ecosystem-Atmosphere Study (BOREAS) was to use remotely sensed observations to estimate GPP and net primary production (NPP) at the spatial resolution of the Advanced Very High Resolution Radiometer (AVHRR) Local Area Coverage (LAC) for the entire BOREAS region. Higher resolution maps would be possible with, e.g., Earth Observing System (EOS) instruments (launched 1998) or with sensors on aircraft platforms. The advantage of satellite data was that, once the component models were validated, consistent measurements could be made across the entire region. Thus, this approach captured gradients of land use intensity and climate. In addition to NPP and GPP, Boreal-PEM provided the data needed to model above-ground biomass and canopy conductance (e.g., maps of air temperature, vapor pressure deficit (VPD), etc.). In combination with land cover and deforestation maps, the remotely sensed measurements of NPP can yield estimates of the impact of land cover change on carbon storage, which is a focus of the follow-on work.

### 1.4 Summary of Parameters

A number of surface variables required to implement Boreal-PEM are retrieved on a daily basis using surface "parameter retrieval" algorithms. These include surface radiometric temperature (Ts), ambient air temperature (Ta), atmospheric precipitable water vapor amount (U), surface absolute humidity, VPD, fractional PAR absorption (FPAR), APAR, standing above-ground biomass, and a cumulative surface wetness index (CSI). Other variables related to the efficiency of light utilization, or the carbon yield of APAR, include the proportion of vegetation cover types that utilize the C3 or C4 photosynthetic pathways. This is derived using long-term climatological information and modeled biomass.

### 1.5 Discussion

Boreal-PEM consists of linked models of canopy radiative transfer, canopy utilization of APAR, and physical environmental variables that have a multiplicative effect on stomatal control. The model is entirely driven with satellite-retrieved surface variables (e.g., APAR, air temperature, soil moisture, absolute humidity, etc.). The resulting "stressed" GPP is reduced to NPP through carbon expenditures associated with autotrophic respiration derived from standing above-ground biomass. The model results closely approximated surface measurements of both physical and biological variables, including NPP, within the BOREAS study areas and were clearly associated with land cover type (i.e., broadleaf deciduous, needleleaf evergreen, etc.).

### 1.6 Related Data Sets

BOREAS Level-3b AVHRR-LAC Imagery: Scaled At-sensor Radiance in LGSOWG Format
BOREAS Level-4b AVHRR-LAC Ten-Day Composite Images: At-sensor Radiance
BOREAS Level-4c AVHRR-LAC Ten-Day Composite Images: Surface Parameters
BOREAS RSS-04 1994 Southern Study Area Jack Pine LAI and FPAR Data
BOREAS RSS-07 Regional LAI and FPAR Images From Ten-Day AVHRR-LAC Composites
BOREAS RSS-14 Level-1 GOES-7 Visible, IR and Water-vapor Images
BOREAS RSS-14 Level-1a GOES-7 Visible, IR, and Water-vapor Images
BOREAS RSS-14 Level-2 GOES-7 Shortwave and Longwave Radiation Images
BOREAS RSS-14 Level-1 GOES-8 Visible, IR and Water-vapor Images
BOREAS RSS-14 Level-1a GOES-8 Visible, IR and Water-vapor Images

## 2. Investigator(s)

### 2.1 Investigator(s) Name and Title

Samual N. Goward (PI), Professor and Chair
Stephen D. Prince, Professor
Scott J. Goetz, Research Scientist
Kevin Czajkowski, Research Scientist
Ralph O. Dubayah, Assoc. Professor

### 2.2 Title of Investigation

Biospheric Dynamics in the Boreal Forest Ecotone

### 2.3 Contact Information


**Contact 1:**
Dr. Scott J. Goetz
Dept. of Geography
University of Maryland
College Park, MD 20742-8225
(301) 405-1297
(301) 314-9299 (fax)
sgoetz@geog.umd.edu.

**Contact 2:**
Samual N. Goward
Dept. of Geography
University of Maryland
College Park, MD 20742-8225
sg21@umail.umd.edu

**Contact 3:**
Stephen D. Prince
Dept. of Geography
University of Maryland
College Park, MD 20742-8225
sp43@umail.umd.edu

**Contact 4:**
Kevin Czajkowski
Dept. of Geography
University of Maryland
College Park, MD 20742-8225
kczajkow@geog.umd.edu

**Contact 5:**
Ralph O. Dubayah
Dept. of Geography
University of Maryland
College Park, MD 20742-8225
rdubayah@geog.umd.edu

**Contact 6:**
Andrea Papagno
Raytheon ITSS
NASA GSFC
Code 923
Greenbelt, MD 20771
(301) 286-3134
(301) 286-0239 (fax)
Andrea.Papagno@gsfc.nasa.gov

# 3. Theory of Measurements

The model is driven primarily by vegetation light absorption, which determines potential photosynthetic rates. The potential rates are reduced by stress terms, including Ta, VPD, and CSI, which act on stomatal physiology (i.e., conductance, Gs). The "stressed" photosynthetic rates are used to provide an actual value of daily carbon gain. The loss of carbon via autotrophic respiration (Ra) is modeled based on a semi-empirical relationship with standing above-ground biomass, which, in turn, is derived from monthly minimum visible reflectance. A contextural approach is used to derive pixel-by-pixel maps of the environmental variables on a daily basis for all days when AVHRR scenes were available (the BOREAS results were based on 35 acquisitions throughout the 1994 growing season). GPP, NPP, Ra, and the amount of NPP per unit APAR on an annual basis are also generated as output maps.

Variations of the PEM approach have been taken by various investigators, beginning with correlative models first described by Kumar and Monteith (1982), Tucker et al. (1983), and Asrar et al. (1985). The Carnegie Ames Stanford Approach (CASA) (Potter et al., 1993) was the first model to use the PEM concept on a global scale, and Global PEM (GLO-PEM) was the first PEM to utilize variables retrieved entirely with remotely sensed observations on a global scale. Descriptions of individual model components and their performance have been reported in numerous journal publications (see Section 10.2.1).

# 4. Equipment

## 4.1 Sensor/Instrument Description

See associated data set documentation in Section 1.6.

### 4.1.1 Collection Environment

See associated data set documentation in Section 1.6.

### 4.1.2 Source/Platform

See associated data set documentation in Section 1.6.

### 4.1.3 Source/Platform Mission Objectives

See associated data set documentation in Section 1.6.

### 4.1.4 Key Variables

See associated data set documentation in Section 1.6.

### 4.1.5 Principles of Operation

See associated data set documentation in Section 1.6.

### 4.1.6 Sensor/Instrument Measurement Geometry

See associated data set documentation in Section 1.6.

### 4.1.7 Manufacturer of Sensor/Instrument

See associated data set documentation in Section 1.6.

## 4.2 Calibration

### 4.2.1 Specifications

See associated data set documentation in Section 1.6.

#### 4.2.1.1 Tolerance
See associated data set documentation in Section 1.6.

### 4.2.2 Frequency of Calibration
See associated data set documentation in Section 1.6.

### 4.2.3 Other Calibration Information
See associated data set documentation in Section 1.6.

# 5. Data Acquisition Methods

All data are recovered with algorithms driven by optical and thermal AVHRR observations, with the exception of incident PAR, which is derived from the Geostationary Operational Environmental Satellite (GOES) observations (provided by Eric Smith for BOREAS).

# 6. Observations

## 6.1 Data Notes
The AVHRR data as provided by the Canada Centre for Remote Sensing (CCRS) to BOREAS were used for these analyses. No additional screening was necessary; however, Boreal-PEM utilizes a series of routines to test for the presence of subpixel clouds, and this technique was improved using the BOREAS data set (Czajkowski et al., 1997a).

## 6.2 Field Notes
None given.

# 7. Data Description

## 7.1 Spatial Characteristics

### 7.1.1 Spatial Coverage
The nominal spatial resolution of the data was 1.1 km at nadir. All data were resampled to 1-km resolution using image mapping techniques developed at CCRS (called GEOCOMP) and validated at the University of Maryland (Czajkowski et al., 1997b).

The corners of the total area covered by the model are defined by the following:

```
  BOREAS Grid          NAD83 Coordinates
X (KM)    Y (KM)      Longitude   Latitude
--------  -------     ----------  ---------
 175.000     0.000    108.51193W  50.97184N
 175.000  1000.000    107.87384W  59.94373N
 975.000     0.000     97.31119W  50.13370N
 975.000  1000.000     93.92214W  58.89897N
```

The total area covered by the model runs was 800 km by 1,000 km, corresponding to the BOREAS study region within the BOREAS Information System (BORIS) X grid range of 175-975 km and the BORIS Y grid range of 0-1000 km, encompassing both the Northern Study Area (NSA) and the Southern Study Area (SSA).

Image coordinates (upper left origin) are easily related to BORIS grid coordinates (lower left origin):

grid_X = image_pixel
grid_Y = 1000 - image_line

For example, the NSA old jack pine tower site (T7Q8T) with BORIS grid coordinates Y=617, X=769 has image coordinates of line=383, pixel=769.

### 7.1.2 Spatial Coverage Map

Not available.

### 7.1.3 Spatial Resolution

All data were resampled by CCRS to 1-km pixels before being used as model input fields.

### 7.1.4 Projection

The area mapped is projected in the BOREAS grid projection, which is based on the ellipsoidal version of the Albers Equal-Area Conic (AEAC) projection. The projection has the following parameters:

```
Datum:        NAD83
Ellipsoid:    GRS80   or WGS84
Origin:       111.000°W  51.000°N
Standard Parallels:      52°  30' 00"N
                         58°  30' 00"N
Units of Measure:  kilometers
```

### 7.1.5 Grid Description

Lines and pixels increase from the upper left corner of the image.

## 7.2 Temporal Characteristics

### 7.2.1 Temporal Coverage

The 34 AVHRR acquisitions defined the observational period during the growing season. The earliest image was 16-Apr-1994 and the latest was 07-Sep-1994. GPP, Ra, and NPP for periods between acquisitions were interpolated to a daily interval using linear interpolation. Annual (growing season) results are summed daily values.

### 7.2.2 Temporal Coverage Map

Not applicable.

### 7.2.3 Temporal Resolution

The model operates on a daily time-step. But the data represent annual values.

### 7.3 Input Data Characteristics

Input data required by the model are summarized in the following table.

**Table 1. Boreal-PEM input variables**

| 7.3.1 Input Parameter/ Variable | 7.3.2 Variable Description/ Definition | 7.3.3 Unit of Measurement | 7.3.4 Data Source | 7.3.5 Data Range |
|---|---|---|---|---|
| visible | spectral exoatmospheric reflectance | % | AVHRR channel 1 | 0, 25 |
| near infrared | spectral exoatmospheric reflectance | % | AVHRR channel 2 | 0, 50 |
| T4 | thermal emission (brightness temperature) | degrees C | AVHRR channel 4 | 0, 50° |
| T5 | thermal emission (brightness temperature) | degrees C | AVHRR channel 5 | 0, 50° |
| NDVI | normalised difference vegetation index | unitless | (ch2-ch1) / (ch2+ch1) | 0, 1 |
| mean Ta | climatological mean air temperature | degrees C | Leemans and Cramer | 0, 50° |
| incident PAR | incident photosynthetically active radiation | MJ/day | GOES (Eric Smith/BORIS) | 0, 12 |
| e | surface spectral emissivity | unitless | Prabhakara and Dalu | 0, 1 |

### 7.4 Output Data Characteristics

Model output is image format, binary single byte-per-pixel (i.e., 8-bit) values that range between 0-255. See Section 8.2 for data format, scaling, and coordinate information. The following table describes the output variables.

**Table 2. Boreal-PEM output variables**

| 7.4.1 Output Parameter Variable | 7.4.2 Variable Description Definition | 7.4.3 Unit of Measurement | 7.4.4 Data Source | 7.4.5 Data Range |
|---|---|---|---|---|
| Ts | surface radiometric temperature | degrees C | modeled | 0, 50° |
| Ta | ambient air temperature | degrees C | modeled | 0, 50° |
| VPD | vapor pressure deficit | millibars (mb) | modeled | 0, 50 |
| CSI | cumulative surface wetness index | unitless | modeled | -5, 5 |
| APAR | absorbed photosynthetically active radiation | megajoules (MJ) | modeled | 0, 12 / day<br>100, 1100 / yr |

| | | | | |
|---|---|---|---|---|
| W | standing above-ground biomass | kg / $m^2$ | modeled | 0, 40 |
| GPP* | gross primary production | $gC/m^2$ | modeled | 0, 40 / day<br>0, 1900 / yr |
| Ra* | autotrophic respiration | $gC/m^2$ | modeled | 0, 35 / day<br>0, 1100 / yr |
| NPP* | net primary production | $gC/m^2$ | modeled | 0, 20 / day<br>0, 850 / yr |
| e* | carbon yield of APAR | gC/MJ | modeled | 0, 1.25 |

* annual images provided to BORIS

### 7.5 Sample Data Record
Not applicable to image data.

## 8. Data Organization

### 8.1 Data Granularity
The smallest unit of data tracked by BORIS was the entire set of images.

### 8.2 Data Format(s)

#### 8.2.1 Uncompressed Data Files
The entire data set contains one American Standard Code for Information Interchange (ASCII) header file and six image files. Each image file contains 1,000 records (image lines) that contain 800 1-byte pixel values.

| File Num. | Description | Record Size | # Records | Bytes/Pixel |
|---|---|---|---|---|
| 1 | ASCII header file | 80 | 11 | N/A |
| 2 | APAR Image | 800 | 1000 | 1 |
| 3 | Biomass Image | 800 | 1000 | 1 |
| 4 | Gross Primary Production | 800 | 1000 | 1 |
| 5 | Light Use Efficiency | 800 | 1000 | 1 |
| 6 | Net Primary Production | 800 | 1000 | 1 |
| 7 | Autotrophic Respiration | 800 | 1000 | 1 |

The image files values must be multiplied or divided by a scaling factor to obtain physical units. The appropriate factors are:

- apar - multiply image values by 4 for actual range of 0 - 900 $gC/m^2$-yr
- biomass - multiply image values by 6 for actual range of 0 - 40 $kg/m^2$
- gpp - multiply image values by 6 for actual range of 0 - 1500 $gC/m^2$-yr
- lue - divide image values by 255 for actual range of 0 - 1 gC/MJ
- npp - multiply image values by 3 for actual range of 0 - 600 $gC/m^2$-yr
- resp - multiply image values by 4 for actual range of 0 - 900 $gC/m^2$-yr

### 8.2.2 Compressed CD-ROM Files

On the BOREAS CD-ROMs, files 2 through 7 listed in Section 8.2.1 have been compressed with the Gzip compression program (file name *.gz). These data have been compressed using gzip version 1.2.4 and the high compression (-9) option (Copyright (C) 1992-1993 Jean-loup Gailly). Gzip (GNU zip) uses the Lempel-Ziv algorithm (Welch, 1994) used in the zip and PKZIP programs. The compressed files may be uncompressed using gzip (-d option) or gunzip. Gzip is available from many Web sites (for example, ftp site prep.ai.mit.edu/pub/gnu/gzip-*.*) for a variety of operating systems in both executable and source code form. Versions of the decompression software for various systems are included on the CD-ROMs.

# 9. Data Manipulations

## 9.1 Formulae

See Section 9.1.1.

### 9.1.1 Derivation Techniques and Algorithms

$$T_s = 1.274 + \left(\frac{e'}{2}\right)T_4 + \left(\frac{e''}{2}\right)T_5 \qquad (1)$$

(after Becker and Li, 1990)

where: $T_4$ = apparent temperature in AVHRR channel 4 (K)
$T_5$ = apparent temperature in AVHRR channel 5 (K)
e = surface spectral emissivity;

$$e = \left(\frac{1-e^*}{0.6}\right)*NDVI + \left(e^* - \left[\frac{0.05(1-e^*)}{0.6}\right]\right) \qquad (2)$$

e* = 'grey-body' emissivity for unvegetated surface (Prabhakara et al., 1977). and e', e" are terms to characterize between-band differences in e.

$$Ta = a * 0.7 + b \qquad (3)$$

where: a = slope of Ts/NDVI relationship
b = intercept of Ts/NDVI relationship
Ta = intercept

where NDVI = 0.7 a,b change with moving window contextural linear regression (TVX) approach.

VPD = vapor pressure deficit (D);

$$D = 0.611*\left[\exp\left(17.27 * \frac{T_a}{T_a + 237}\right) - \exp\left(17.27 * \frac{T_d}{T_d + 237}\right)\right] \qquad (4)$$

where $T_d$ = dewpoint temperature;

$$T_d = \frac{\ln(\lambda+1) + \ln(U) - 0.1133}{0.0393} \qquad (5)$$

and I = coefficient to adjust for latitude and season (Smith 1966).
U = atmospheric precipitable water content (cm);

$$U = 17.32 * \frac{(DT - 0.6831)}{(TS - 291.97)} + 0.5456 \quad (6)$$

and DT = T4-T5

CSI = cumulative surface wetness index (Sg);

$$\Sigma\gamma = \Sigma\gamma_{t-1} + \gamma_t \quad (7)$$

where $g_t$ = slope of Ts/NDVI at time (t) (i.e., a simple 'bucket' model in which $g_t$, corrected for solar zenith angle effects, varies relative to a normalized value, 0.5);

APAR = absorbed photosynthetically active radiation,

$$APAR = FPAR * PAR \quad (8)$$

where: FPAR = 1.67*NDVI - 0.08
NDVI = (ch2-ch1)/(ch2+ch1)
PAR = incident PAR from GOES (E. Smith/BORIS)

NPP = net primary production;

$$NPP = GPP - Ra \quad (9)$$

GPP = gross primary production;

$$GPP = APAR * e_g \quad (10a)$$

where $e_g = e_g{}^*$ (modified by multipliers that simulate stomatal physiology, Gs); i.e., Ta, VPD, CSI)

$$\varepsilon_g^* = 55.2\alpha \quad (10b)$$

$\alpha$ = quantum yield of photosynthesis (Collatz, et al. 1991)

$e_n$ = carbon yield of APAR (g/MJ);

$$e_n = NPP / APAR \quad (11)$$

Ra = autotrophic respiration;

$$Ra = \left[\left(\frac{0.4}{0.75}\right) * \left(\frac{10^3}{10^3 W + 50}\right)\right] \quad (12)$$

W = standing aboveground biomass;

$$W = 7166.1 \left(\rho^{-2.6}\right) \quad 13)$$

r = minimized visible reflectance (ch1) on an annual basis, cloud-screened and corrected for sun angle

## 9.2 Data Processing Sequence

### 9.2.1 Processing Steps

Each individual AVHRR image is input to the model, and the various component models derive intermediate products that are then interpolated to a daily basis and integrated annually. The full processing sequence is complex because of the availability of individual AVHRR acquisitions, the number of individual component algorithms, and the exchange of variables between the different model time-steps. A sense of the processing steps can be best acquired in Prince and Goward (1995), Goetz et al. (1998), and the flowchart below.

BORIS staff copied the ASCII and compressed the binary files for release on CD-ROM.

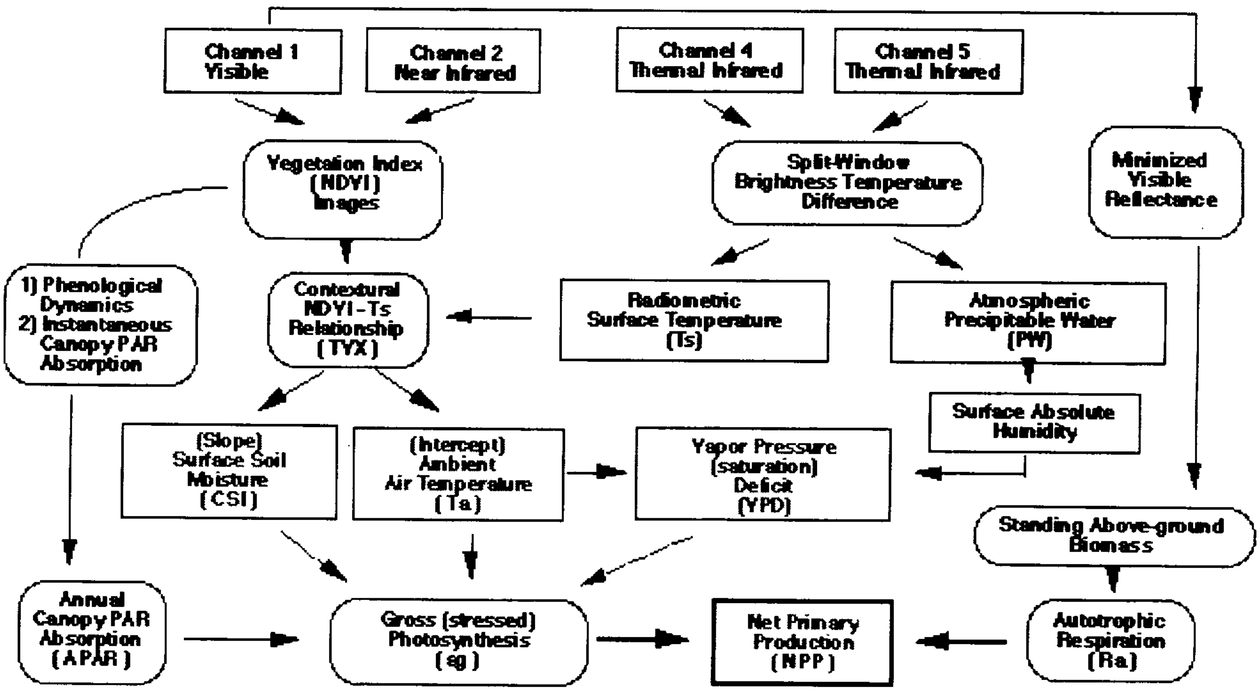


### 9.2.2 Processing Changes

None given.

## 9.3 Calculations

### 9.3.1 Special Corrections/Adjustments

None.

### 9.3.2 Calculated Variables

See Table 2.

## 9.4 Graphs and Plots

For BOREAS-specific results see Goetz and Prince (1998).

# 10. Errors

## 10.1 Sources of Error

There are several potential sources of error that can affect the model results. These include errors in the data that drive the model (e.g., calibration and correction of the AVHRR reflectances and temperatures, the GOES PAR maps and their time-integration), errors in the recovery of surface variables within model component algorithms (e.g., Ts, Ta, U, VPD, FPAR, APAR, W, en, etc.), and multiplicative or canceling errors in variables derived from other recovered variables and parameters (e.g., APAR, Ra, GPP, NPP, etc.).

## 10.2 Quality Assessment

### 10.2.1 Model Validation by Source

Numerous journal articles describe efforts to test, compare, and validate various component model results. The validity of physical environmental components of the model (i.e., Ts, Ta, U, VPD, CSI) have been assessed with different field experiment data (SNF, FIFE, HAPEX-Sahel, OTTER, GEWEX, BOREAS) as listed in the following table (see acronym list, Section 19).

| Author(s) | Variables | Field Data |
|---|---|---|
| Czajkowski et al. (1997a) | Ta | BOREAS |
| Goetz (1997) | CSI | FIFE |
| Goetz et al. (1998) | CSI | BOREAS |
| Goward et al. (1994) | Ta, U, VPD, CSI | OTTER |
| Goward and Dye (1997) | Ta, U, VPD, CSI | Global |
| Prihodko and Goward (1997) | Ta | FIFE |
| Prince and Goward (1995) | Ta, U, VPD, CSI | Global |
| Prince et al. (1998) | Ts, Ta, U, VPD | FIFE, HAPEX, GEWEX, BOREAS |

The biological components of the model have been assessed in the following journal publications:

**Validation of biological components of Boreal-PEM.**

| Author(s) | Variables | Field Data |
|---|---|---|
| Goetz and Prince (1996, 1998) | $e_n$, $e_g$, $e_g$*, NPP, GPP, Ra, APAR | SNF |
| Goetz et al. (1998) | $e_n$, NPP, GPP, Ra | BOREAS |
| Goward et al. (1994) | FPAR, APAR | OTTER |
| Hanan et al. (1995, 1997) | $e_n$, $g_s$, NPP, Ra, FPAR, APAR | HAPEX-Sahel |
| Prince and Goward (1995) | $e_n$, $e_g$, NPP, GPP, Ra, FPAR, APAR | Global |
| Prince et al. (1995) | $e_n$, $e_g$, NPP, Ra, APAR | SNF, Global |

Numerous other articles have examined more general aspects of model components (particularly with respect to Ts and U). A brief summary of results from the previous tables is provided below in Sections 10.2.2-10.2.4.

### 10.2.2 Confidence Level/Accuracy Judgment

Confidence in the results is very high in terms of the spatial patterns and magnitudes within the images and moderate to high in terms of the absolute values of variables recovered (see Sections 10.2.3 and 10.2.4). Comparisons showed a close correspondence between measured and inferred soil moisture at the BOREAS sites. There was also good agreement between inferred and site measurements of biomass and NPP, although the biomass values were underestimated compared to those derived with an independent technique (i.e., Hall et al., 1995).

### 10.2.3 Measurement Error for Variables

In quantitative terms, the results of model component validation work showed that Ts could be retrieved with root mean square (RMS) errors of 3.5 °C for a range of 48 °C; Ta with 3.9 °C over a range of 36 °C; U with 0.6 cm over a range of 3.6 cm; and VPD with 10.9 mb over a range of 58 mb (Prince et al., 1998). There was some evidence of compounding errors in VPD because of the integration of multiple retrieved variables (Ts, Ta, U). FPAR was recovered with an RMS error of 2.4% over a wide range of sites in Oregon (Goward et al., 1994). There was some evidence of a lag between the CSI and soil moisture at depth at sites in Oregon. The CSI was found to predict surface soil moisture at a grassland site in central Kansas with an RMS error of 3.2% (Goetz, 1997).

### 10.2.4 Additional Quality Assessments

Although the results sometimes had low absolute accuracies, the field data themselves are not without error: although the inferences were usually for a >1 $km^2$ area made instantaneously, they were compared with point field values generally not measured at exactly the same times in the day or covering the same spatial area. Maps of retrieved variables had good relative accuracy and possibly better absolute accuracy than the comparisons with point measurements suggest.

### 10.2.5 Data Verification by Data Center

Data were examined for general consistency and clarity.

## 11. Notes

### 11.1 Limitations of the Data

The model is probably limited in terms of Ra recovery; hence NPP, because of the potential insensitivity of Ra to biomass in boreal forest stands (Goetz and Prince, 1998).

### 11.2 Known Problems with the Data

None.

### 11.3 Usage Guidance

Before uncompressing the Gzip files on CD-ROM, be sure that you have enough disk space to hold the uncompressed data files. Then use the appropriate decompression program provided on the CD-ROM for your specific system.

### 11.4 Other Relevant Information

Contact Dr. Scott J. Goetz for a platform-independent version of the model that is available; however, the model is highly system-tailored and requires 50 Gigabytes of space for a single run. If someone really wants it, Dr. Goetz could discuss with them some collaborative effort to get it functioning in another lab.

## 12. Application of the Data Set

The model may be operated with any remotely sensed observations that provide a measure of vegetation amount (e.g., spectral vegetation indices) and thermal emission in more than one channel (in order to get split-window surface radiometric temperature). The results are applicable to many studies, from characterizing carbon flux and storage over large areas to monitoring changes in forest productivity, stress, and management.

# 13. Future Modifications and Plans

A heterotrophic respiration (Rh) component is being added to the model in order to simulate, when combined with NPP, net ecosystem productivity (NEP). Simulated NEP is more directly comparable with eddy correlation (e.g., tower) carbon flux measurements than is NPP because of the lack of separability between the Ra and Rh components of measured soil $CO_2$ efflux. Moreover, NEP is important to characterize in order to quantify the direction of vegetation - atmosphere fluxes and to address carbon budgets at the local to global scale.

# 14. Software

## 14.1 Software Description

Version 1 of the model was developed and operated under the PCI image processing package using the Engineering Analysis and Scientific Interface (EASI) procedure language. The model has since been exported, primarily for speed of processing and modularity, to the UNIX environment. Version 2 is written in the C programming language. Version 2 is operable and changes to the model are reported in the upcoming publication Goetz et al. (1999a). BOREAS results with version 2 of the model are reported in Goetz et al. (1999b).

Gzip (GNU zip) uses the Lempel-Ziv algorithm (Welch, 1994) used in the zip and PKZIP commands.

## 14.2 Software Access

Contact Dr. Scott J. Goetz for a platform-independent version of the model that is available, however the model is highly system-tailored and requires 50 Gigabytes of space for a single run. If someone really wants it, Dr. Goetz could discuss with them some collaborative effort to get it functioning in another lab.

Gzip is available from many Web sites across the Internet (for example, ftp site prep.ai.mit.edu/pub/gnu/gzip-*.*) for a variety of operating systems in both executable and source code form. Versions of the decompression software for various systems are included on the CD-ROMs.

# 15. Data Access

The production efficiency model images are available from the Earth Observing System Data and Information System (EOSDIS) Oak Ridge National Laboratory (ORNL) Distributed Active Archive Center (DAAC).

## 15.1 Contact Information

For BOREAS data and documentation please contact:

ORNL DAAC User Services
Oak Ridge National Laboratory
P.O. Box 2008 MS-6407
Oak Ridge, TN 37831-6407
Phone: (423) 241-3952
Fax: (423) 574-4665
E-mail: ornldaac@ornl.gov or ornl@eos.nasa.gov

### 15.2 Data Center Identification

Earth Observing System Data and Information System (EOSDIS) Oak Ridge National Laboratory (ORNL) Distributed Active Archive Center (DAAC) for Biogeochemical Dynamics http://www-eosdis.ornl.gov/.

### 15.3 Procedures for Obtaining Data

Users may obtain data directly through the ORNL DAAC online search and order system [http://www-eosdis.ornl.gov/] and the anonymous FTP site [ftp://www-eosdis.ornl.gov/data/] or by contacting User Services by electronic mail, telephone, fax, letter, or personal visit using the contact information in Section 15.1.

### 15.4 Data Center Status/Plans

The ORNL DAAC is the primary source for BOREAS field measurement, image, GIS, and hardcopy data products. The BOREAS CD-ROM and data referenced or listed in inventories on the CD-ROM are available from the ORNL DAAC.

## 16. Output Products and Availability

### 16.1 Tape Products

None.

### 16.2 Film Products

None.

### 16.3 Other Products

These images are available on the BOREAS CD-ROM series.

Output image products listed in Section 7.4, Table 2, and described herein, that are not included on the BOREAS CD-ROM might be available on request.

A description of the model, summary of research papers, and results of model application at the global scale are available at the following URL: http://www.geog.umd.edu/glopem/.

## 17. References

### 17.1 Platform/Sensor/Instrument/Data Processing Documentation

Thawley, M. and J. Small. 1997. The Global Production Efficiency Model, version 2.0 (GLO-PEM2).

Welch, T.A. 1984. A Technique for High Performance Data Compression. IEEE Computer, Vol. 17, No. 6, pp. 8-19.

### 17.2 Journal Articles and Study Reports

Asrar, G., E.T. Kanemasu, R.D. Jackson, and P.J. Pinter. 1985. Estimation of total above ground phytomass production using remotely sensed data. Remote Sensing of Environment, 17: 211-220.

Becker, F. and Z.L. Li. 1990. Towards a local split window method over land surfaces. International Journal of Remote Sensing, 11: 1509-1522.

Collatz, G.J., J.T. Ball, C. Grivet, and J.A. Berry. 1991. Physiological and environmental regulation of stomatal conductance, photosynthesis and transpiration: a model that includes a laminar boundary layer. Agricultural and Forest Meteorology, 54: 107-136.

Czajkowski, K.P., T. Mulhern, S.N. Goward, J. Cihlar, R.O. Dubayah, and S.D. Prince. 1997a. Biospheric environmental monitoring at BOREAS with AVHRR observations. Journal of Geophysical Research, 102 (D24): 29,651-29,662.

Czajkowski, K.P., T. Mulhern, S.N. Goward, and J. Cihlar. 1997b. Validation of the geocoding and compositing system (GEOCOMP) using contextural analysis for AVHRR images. International Journal of Remote Sensing, 18 (14): 3055-3068.

Goetz, S.J. 1997. Multi-sensor analysis of NDVI, surface temperature, and biophysical variables at a mixed grassland site. International Journal of Remote Sensing, 18: 71-94.

Goetz, S.J. and S.D. Prince. 1996. Remote sensing of net primary production in boreal forest stands. Agricultural and Forest Meteorology, 78: 149-179.

Goetz, S.J. and S.D. Prince. 1998. Variability in carbon exchange and light utilization among boreal forest stands: implications for remote sensing of net primary production. Canadian Journal of Forest Research 28: 375-389.

Goetz, S.J. and S.D. Prince. 1999. Modeling terrestrial carbon exchange and storage: the evidence for and implications of functional convergence in light use efficiency. Advances in Ecological Research, 28: 57-92.

Goetz, S.J., S.D. Prince, M.M. Thawley, K.P. Czajkowski, and S.N. Goward. 1999. Mapping regional patterns of canopy carbon exchange and storage with remote sensing. Journal of Geophysical Research (in press).

Goetz, S.J., S.D. Prince, S.N. Goward, M. Thawley, and J. Small. 1999a. Satellite remote sensing of primary production: an improved production efficiency modeling approach. Ecological Modeling (in press).

Goetz, S.J., S.D. Prince, S.N. Goward, M.M. Thawley, J. Small, and A. Johnston. 1999b. Mapping net primary production and related biophysical variables with remote sensing: application to the BOREAS region. Journal of Geophysical Research (in press).

Goward, S.N. and D.G. Dye. 1997. Global biospheric monitoring with remote sensing. In: The use of remote sensing in modeling forest productivity (eds. H.L. Gholtz, K. Nakane, and H. Shimoda). pages 241-272, Kluwer Academic, New York.

Goward, S.N., R.H. Waring, and D.G. Dye. 1994. Ecological remote sensing at OTTER: Macroscale satellite observations. Ecological Applications, 4: 322-343.

Hall, F.G., Y. Shimabukuro, and K.F. Huemmrich. 1995. Remote sensing of forest biophysical structure in boreal stands of Picea mariana using mixture decomposition and geometric reflectance models. Ecological Applications, 5: 993-1013.

Hanan, N.P., S.D. Prince, and A. Bègué. 1995. Estimation of absorbed photosynthetically active radiation and vegetation net production efficiency using satellite data. Agricultural and Forest Meteorology, 76: 259-276.

Hanan, N.P., S.D. Prince, and A. Bègué. 1997. Modelling vegetation primary production during HAPEX-Sahel using production efficiency and canopy conductance model formulations. Journal of Hydrology, 188/189: 651-675.

Kumar, M. and J.L. Monteith. 1982. Remote sensing of plant growth. In: Plants and the Daylight Spectrum (eds. H. Smith), pp. 133-144. Academic Press, London.

Leemans, R. and W.P. Cramer. 1991. The IISAS database for mean monthly values of temperature, precipitation and cloudiness on a global terrestrial grid, Laxenburg, Austria International Institute for Applied Systems Analysis.

Newcomer, J., D. Landis, S. Conrad, S. Curd, K. Huemmrich, D. Knapp, A. Morrell, J. Nickeson, A. Papagno, D. Rinker, R. Strub, T. Twine, F. Hall, and P. Sellers, eds. 2000. Collected Data of The Boreal Ecosystem-Atmosphere Study. NASA. CD-ROM.

Potter, C.S., J.T. Randerson, C.B. Field, P.A. Matson, P.M. Vitousek, H.A. Mooney, and S.A. Klooster. 1993. Terrestrial ecosystem production: A process model based on global satellite and surface data. Global Biogeochemical Cycles, 7: 811-841.

Prabhakara, C., G. Dalu, R.C. Lo, and R. Nath. 1977. Remote sensing of seasonal distribution of precipitable water over the oceans and inference of boundary layer structure. Monthly Weather Review, 107: 1388-1401.

Prihodko, L. and S.N. Goward. 1997. Estimation of air temperature from remotely sensed observations. Remote Sensing of Environment, 60: 335-346.

Prince, S.D. and S.J. Goward. 1995. Global primary production: a remote sensing approach. Journal of Biogeography, 22: 815-835.

Prince, S.D., S.J. Goetz, and S.N. Goward. 1995. Monitoring primary production from Earth observing satellites. Water, Air, and Soil Pollution, 82: 509-522.

Prince, S.D., S.J. Goetz, K. Czajkowski, R. Dubayah, and S.N. Goward. 1998. Inference of surface and air temperature, atmospheric precipitable water and vapor pressure deficit using AVHRR satellite observations: validation of algorithms. Journal of Hydrology, 213 (1-4), 230-249.

Sellers, P. and F. Hall. 1994. Boreal Ecosystem-Atmosphere Study: Experiment Plan. Version 1994-3.0, NASA BOREAS Report (EXPLAN 94).

Sellers, P. and F. Hall. 1996. Boreal Ecosystem-Atmosphere Study: Experiment Plan. Version 1996-2.0, NASA BOREAS Report (EXPLAN 96).

Sellers, P., F. Hall, and K.F. Huemmrich. 1996. Boreal Ecosystem-Atmosphere Study: 1994 Operations. NASA BOREAS Report (OPS DOC 94).

Sellers, P., F. Hall, and K.F. Huemmrich. 1997. Boreal Ecosystem-Atmosphere Study: 1996 Operations. NASA BOREAS Report (OPS DOC 96).

Sellers, P., F. Hall, H. Margolis, B. Kelly, D. Baldocchi, G. den Hartog, J. Cihlar, M.G. Ryan, B. Goodison, P. Crill, K.J. Ranson, D. Lettenmaier, and D.E. Wickland. 1995. The boreal ecosystem-atmosphere study (BOREAS): an overview and early results from the 1994 field year. Bulletin of the American Meteorological Society. 76(9):1549-1577.

Sellers, P.J., F.G. Hall, R.D. Kelly, A. Black, D. Baldocchi, J. Berry, M. Ryan, K.J. Ranson, P.M. Crill, D.P. Lettenmaier, H. Margolis, J. Cihlar, J. Newcomer, D. Fitzjarrald, P.G. Jarvis, S.T. Gower, D. Halliwell, D. Williams, B. Goodison, D.E. Wickland, and F.E. Guertin. 1997. BOREAS in 1997: Experiment Overview, Scientific Results and Future Directions. Journal of Geophysical Research 102(D24): 28,731-28,770.

Smith, W.L. 1966. Note on the relationship between precipitable water and surface dew point. Journal of Applied Meteorology, 5: 726-727.

Tucker, C.J., C.L. Vanpraet, E. Boerwinkel, and A. Gaston. 1983. Satellite remote sensing of total dry matter accumulation in the Senegalese Sahel. Remote Sensing of Environment, 13: 461-474.

### 17.3 Archive/DBMS Usage Documentation

None.

## 18. Glossary of Terms

CSI - Cumulative surface wetness index
Gs - Stomatal conductance
e - Carbon yield of APAR
Ra - Autotrophic respiration
Rh - Heterotrophic respiration
Ta - Ambient air temperature
Ts - Surface radiometric temperature
U - Atmospheric precipitable water vapor amount
W - Standing above-ground biomass

## 19. List of Acronyms

APAR - Absorbed Photosynthetically Active Radiation
ASCII - American Standard Code for Information Interchange
AVHRR - Advanced Very High Resolution Radiometer
Boreal-PEM - Boreal Forest Production Efficiency Model
BOREAS - BOReal Ecosystem-Atmosphere Study
BORIS - BOREAS Information System
CASA - Carnegie Ames Stanford Approach
CCRS - Canada Centre Remote Sensing
CD-ROM - Compact Disk-Read-Only memory
DAAC - Distributed Active Archive Center
EASI - Engineering Analysis and Scientific Interface
EOS - Earth Observing System
EOSDIS - EOS Data and Information System
FIFE - First International Satellite Land Surface Climatology Field Experiment
FPAR - Fraction of incident PAR intercepted or absorbed
GEOCOMP - Geocoding and Compositioning System
GEWEX - Global Water Energy and Water Cycle Experiment
GIS - Geographic Information System
GLO-PEM - Global Production Efficiency Model
GOES - Geostationary Operational Environmental Satellite
GPP - Gross Primary Production
GSFC - Goddard Space Flight Center (NASA)
HAPEX-Sahel - Hydrology Atmosphere Pilot Experiment in the Sahel
HTML - HyperText Markup Language
IFC - Intensive Field Campaign
LAC - Local Area Coverage (of AVHRR)
NAD83 - North American Datum of 1983
NASA - National Aeronautics and Space Administration
NDVI - Normalized Difference Vegetation Index

```
NEP          - Net Ecosystem Production
NOAA         - National Oceanic and Atmospheric Administration
NPP          - Net Primary Production
NSA          - Northern Study Area
ORNL         - Oak Ridge National Laboratory
OTTER        - Oregon Transect Experiment
PANP         - Prince Albert National Park
PAR          - Photosynthetically Active Radiation
PEM          - Production Efficiency Model
RMS          - Root Mean Square (Error)
SNF          - Superior National Forest, Minnesota
SSA          - Southern Study Area
TE           - Terrestrial Ecology
TF           - Tower Flux
URL          - Uniform Resource Locator
UTM          - Universal Transverse Mercator
VPD          - Vapor Pressure Deficit
```

# 20. Document Information

## 20.1 Document Revision Date
Written: 25-Jun-1997
Last Updated: 24-Sep-1999

## 20.2 Document Review Date(s)
BORIS Review: 04-May-1999
Science Review: 26-Oct-1998

## 20.3 Document ID

## 20.4 Citation
When using these data, please include the following reference:

Goetz, S.J. and S.D. Prince. 1998. Variability in carbon exchange and light utilization among boreal forest stands: implications for remote sensing of net primary production. Canadian Journal of Forest Research 28: 375-389.

If using data from the BOREAS CD-ROM series, also reference the data as:

Goward, S.N., S.D. Prince, S.J. Goetz, K. Czajkowski, and R.O. Dubayah, "Biospheric Dynamics in the Boreal Forest Ecotone." In Collected Data of The Boreal Ecosystem-Atmosphere Study. Eds. J. Newcomer, D. Landis, S. Conrad, S. Curd, K. Huemmrich, D. Knapp, A. Morrell, J. Nickeson, A. Papagno, D. Rinker, R. Strub, T. Twine, F. Hall, and P. Sellers. CD-ROM. NASA, 2000.

Also, cite the BOREAS CD-ROM set as:

Newcomer, J., D. Landis, S. Conrad, S. Curd, K. Huemmrich, D. Knapp, A. Morrell, J. Nickeson, A. Papagno, D. Rinker, R. Strub, T. Twine, F. Hall, and P. Sellers, eds. Collected Data of The Boreal Ecosystem-Atmosphere Study. NASA. CD-ROM. NASA, 2000.

## 20.5 Document Curator

## 20.6 Document URL

| **REPORT DOCUMENTATION PAGE** | *Form Approved* *OMB No. 0704-0188* |
|---|---|



**1. AGENCY USE ONLY** *(Leave blank)*

**2. REPORT DATE**
October 2000

**3. REPORT TYPE AND DATES COVERED**
Technical Memorandum

**4. TITLE AND SUBTITLE**
Technical Report Series on the Boreal Ecosystem-Atmosphere Study (BOREAS)
BOREAS TE-17 Production Efficiency Model Images

**5. FUNDING NUMBERS**
923
RTOP: 923-462-33-01

**6. AUTHOR(S)**
Scott J. Goetz, Samual N. Goward, Stephen D. Prince, Kevin Czajkowski, and Ralph O. Dubayah
Forrest G. Hall and Andrea Papagno, Editors

**7. PERFORMING ORGANIZATION NAME(S) AND ADDRESS (ES)**
Goddard Space Flight Center
Greenbelt, Maryland 20771

**8. PEFORMING ORGANIZATION REPORT NUMBER**
2000-03136-0

**9. SPONSORING / MONITORING AGENCY NAME(S) AND ADDRESS (ES)**
National Aeronautics and Space Administration
Washington, DC 20546-0001

**10. SPONSORING / MONITORING AGENCY REPORT NUMBER**
TM—2000–209891
Vol. 171

**11. SUPPLEMENTARY NOTES**
S. Goetz, S.N. Goward, S.D. Prince, K. Czajkowski, and R.O. Dubayah: University of Maryland, College Park; A. Papagno: Raytheon ITSS, NASA Goddard Space Flight Center, Greenbelt, Maryland

**12a. DISTRIBUTION / AVAILABILITY STATEMENT**
Unclassified–Unlimited
Subject Category: 43
Report available from the NASA Center for AeroSpace Information, 7121 Standard Drive, Hanover, MD 21076-1320. (301) 621-0390.

**12b. DISTRIBUTION CODE**

**13. ABSTRACT** *(Maximum 200 words)*

A BOREAS version of the Global Production Efficiency Model (http://www.inform.umd.edu/glopem/ [Internet Link]) was developed by TE-17 to generate maps of gross and net primary production, autotrophic respiration, and light use efficiency for the BOREAS region. This document provides basic information on the model and how the maps were generated. The data generated by the model are stored in binary image-format files.

**14. SUBJECT TERMS**
BOREAS, terrestrial ecology.

**15. NUMBER OF PAGES**
19

**16. PRICE CODE**

| 17. SECURITY CLASSIFICATION OF REPORT | 18. SECURITY CLASSIFICATION OF THIS PAGE | 19. SECURITY CLASSIFICATION OF ABSTRACT | 20. LIMITATION OF ABSTRACT |
|---|---|---|---|
| Unclassified | Unclassified | Unclassified | UL |

NSN 7540-01-280-5500

Standard Form 298 (Rev. 2-89)
Prescribed by ANSI Std. Z39.18
298-102